Phosphate starvation response controls genes required to synthesize the phosphate analog arsenate

Authors: Qian Wang, Yoon-Suk Kang, Abdullah Alowaifeer, Kaixiang Shi, Xia Fan, Lu Wang, Jonathan Jetter, Brian Bothner, Gejiao Wang, and Timothy R. McDermott

Wang, Qian, Yoon-Suk Kang, Abdullah Alowaifeer, Kaixiang Shi, Xia Fan, Lu Wang, Jonathan Jetter, Brian Bothner, Gejiao Wang, and Timothy R. McDermott. "Phosphate starvation response controls genes required to synthesize the phosphate analog arsenate." Environmental Microbiology 20, no. 5 (May 2018): 1782-1793. DOI:10.1111/1462-2920.14108.

Phosphate starvation response controls genes required to synthesize the phosphate analog arsenate

Qian Wang,[1,2†§] Yoon-Suk Kang,[2†§] Abdullah Alowaifeer,[2] Kaixiang Shi,[1] Xia Fan,[1] Lu Wang,[1] Jonathan Jetter,[2] Brian Bothner,[3] Gejiao Wang[1*] and Timothy R. McDermott [2]**

[1]*State Key Laboratory of Agricultural Microbiology, College of Life Science and Technology, Huazhong Agricultural University, Wuhan 430070, People's Republic of China.*

[2]*Departments of Land Resources & Environmental Sciences and* [3]*Chemistry and Biochemistry, Montana State University, Bozeman, MT 59717, USA.*

Summary

Environmental arsenic poisoning affects roughly 200 million people worldwide. The toxicity and mobility of arsenic in the environment is significantly influenced by microbial redox reactions, with arsenite (As^{III}) being more toxic than arsenate (As^{V}). Microbial oxidation of As^{III} to As^{V} is known to be regulated by the AioXSR signal transduction system and viewed to function for detoxification or energy generation. Here, we show that As^{III} oxidation is ultimately regulated by the phosphate starvation response (PSR), requiring the sensor kinase PhoR for expression of the As^{III} oxidase structural genes *aioBA*. The PhoRB and AioSR signal transduction systems are capable of transphosphorylation cross-talk, closely integrating As^{III} oxidation with the PSR. Further, under PSR conditions, As^{V} significantly extends bacterial growth and accumulates in the lipid fraction to the apparent exclusion of phosphorus. This could spare phosphorus for nucleic acid synthesis or triphosphate metabolism wherein unstable arsenic esters are not tolerated, thereby enhancing cell survival potential. We conclude that As^{III} oxidation is logically part of the bacterial PSR, enabling the synthesis of the phosphate analog As^{V} to replace phosphorus in specific biomolecules or to synthesize other molecules capable of a similar function, although not for total replacement of cellular phosphate.

Introduction

Microorganisms react robustly with arsenic in nature, catalyzing redox reactions that strongly influence As mobility and toxicity in the environment. These transformations primarily involve arsenite (As^{III}) oxidation and arsenate (As^{V}) reduction, although As methylation also occurs; see recent review by Andres and Bertin (Andres and Bertin, 2016). Different mechanisms control transcriptional up-regulation of relevant genes upon cell exposure to As^{III}. The ArsR repressor regulates expression of genes encoding functions associated with arsenic detoxification (Andres and Bertin, 2016) and As^{V} dissimilatory reduction (Murphy and Saltikov, 2009). For activation of As^{III} oxidase structural genes (*aioBA*), the best studied system involves a three-component signal transduction system comprised of a periplasmic As^{III} binding protein AioX, a histidine sensor kinase AioS and its cognate response regulator AioR (Kashyap *et al.*, 2006; Cai *et al.*, 2009; Liu *et al.*, 2012).

Recent work has unveiled aspects of microbial arsenic metabolism that is poorly studied or even controversial. Specifically, we refer to As^{V} substituting for its chemical analog, phosphate (Pi) (Wolfe-Simon *et al.*, 2011). Studies have shown arsenoesters to be unstable (reviewed by Rosen *et al.*, 2011) and therefore functional $As^{V} \rightarrow$ Pi substitutions involving such bonding (e.g., nucleic acid, ATP) is viewed to not occur. However, As^{V} can be incorporated into arsenosugars and arsenolipids as a methylated pentavalent As-C bond, which is very stable and well documented in higher organisms (Dembitsky and Levitsky, 2004). Arsenic accumulation in bacteria also occurs (Takeuchi *et al.*, 2007; Yan *et al.*, 2014; Wang *et al.*, 2015; Pandey and Bhatt, 2015) and in marine macroalgae is found as arsenohydrocarbons and arsenophospholipids (Francesconi and Kuehnelt, 2002; Francesconi, 2010; Raab *et al.*, 2013). However, understanding why a microorganism accumulates arsenic or how it may use it remains to be understood.

Our joint efforts in studying microbial As^{III} oxidation employ two strains of *Agrobacterium tumefaciens* as models (strains GW4 and 5A). Induction of *aioBA* (encodes the two subunits of the arsenite oxidase enzyme) is influenced by Pi levels in the culture medium (Kang *et al.*, 2012a; Wang *et al.*, 2015) and coordinated in parallel with the expression of alkaline phosphatase (AP), which is the universal endogenous reporter enzyme of the Pi starvation response (PSR) in bacteria. In all Gram-negative bacteria thus far studied, the PSR is regulated via a two-component signal transduction system comprised of the sensor histidine kinase PhoR and its cognate response regulator PhoB. PhoU and PstS are also involved, with the most recent evidence suggesting they interact with PhoR and are involved in de-activating the PSR (Wanner, 1996; Hsieh and Wanner, 2010; diCenzo *et al.*, 2017). In *A. tumefaciens*, induction of an *aioB*::*lacZ* reporter is either undetectable or the kinetics significantly disrupted in Δ*phoB1*, Δ*phoU1* and Δ*pstS1* mutants (Kang *et al.*, 2012a). Similarly, expression of the regulatory genes *aioSR* is also regulated by Pi, failing to be induced by As^{III} in these same *pho*/*pst* mutants (Kang *et al.*, 2012a). As such, the evidence supports the hypothesis that all of the *aio* genes are controlled directly or indirectly by the PhoR-B signal transduction system. This infers a regulatory association between the PSR and the biosynthesis of As^{V}, a known Pi analog. Here, we describe experiments directly showing that regulation of As^{III} oxidation is part of the PSR. As might be predicted if this is of physiological relevance, we also demonstrate that As^{V} will extend growth of Pi starved cells, accumulating in cell lipids to the exclusion of Pi. This illustrates a complete, logical and systematic linkage between a bacterial cell sensing nutrient starvation and a cellular response that constitutes an ecologically cogent reaction to deal with the deprivation.

Results

The orientation and relative position of strategic genes and promoters studied in these experiments are shown in Fig. 1A and B. Deletion mutations (non-polar) were introduced into genes encoding the sensor kinases *aioS* and *phoR* in order to characterize the extent to which they are involved in As^{III} oxidation and or the PSR. In both regulatory mutants, an *aioB*::*lacZ* reporter fusion was used for tracking regulation of As^{III} oxidation, and expression of various *pho* and *pst* reporters were also followed to understand the influence of the phoR and aioS mutations on cell responses related to the PSR and or As^{III} exposure.

AioS and PhoR are essential for As^{III} oxidation

Given the prior reports implicating AioS as a sensor kinase involved in up-regulating the expression of the As^{III} oxidase structural genes *aioBA* (Kashyap *et al.*, 2006; Cai *et al.*, 2009), it was important to use mutational analysis to demonstrate that it is essential for As^{III} oxidation as well as for determining whether it may be involved in the integration of As^{III} with the PSR. Introduction of an Δ*aioS* mutation resulted in a null As^{III} oxidation phenotype (Fig. 1C) and thus was not surprising. However, the null As^{III} oxidation phenotype (Fig. 1C) of the Δ*phoR* represents a novel development because it implicates PhoR as being a major regulatory controller. We then sought to determine if specific amino acids known to be involved in sensor kinase phosphorelay signal transduction are involved. Amino acid replacement mutations involving H210 (predicted canonical phosphorylation site for sensor kinases, Supporting Information Fig. S1) or G359 (predicted HATPase domain, Supporting Information Fig. S1) were incorporated into the PCR cloned *phoR* and to assess whether these mutated alleles would rescue the Δ*phoR* mutant. In contrast to the Δ*phoR* mutant being reverted back to wild type by *phoR* carried in pCPP30, the mutated alleles failed to rescue the negative As^{III} oxidation phenotype (Fig. 1C), providing strong evidence that the role of PhoR in As^{III} oxidation involves gene regulation via the signal transduction pathway documented to govern the PSR (Stock *et al.*, 1989; Gao and Stock,2009).

Subsequent experiments then examined the extent to which AioS and PhoR exert regulatory control over genes essential to As^{III} oxidation as well as genes known to be involved in the bacterial PSR. β-galactosidase reporter constructs for *aioB*, *phoB1*, *pstS1* and *pstS2* were assayed in wild type and in Δ*phoR* and Δ*aioS* mutants. Culture conditions were as we previously described (Kang *et al.*, 2012a) that initiate as non-limiting for Pi, but then transition to a PSR situation as Pi is taken up by cells and triggering expression of *aioB* and AP. Culture conditions also included ± As^{III} treatments to assess potential interactive functions of As^{III}-based signalling.

In the wild type cell and in the absence of As^{III}, *pstS2*::*lacZ* and *phoB1*::*lacZ* up-regulated approximately eight- and five-fold respectively (Fig. 2A; Note, Y-axis scale required to accommodate *pstS2::lacZ* compressing the *phoB1::lacZ* profile) and coincided with culture conditions that yield PSR cells at approximately two hours, corresponding exactly to our prior work (Kang *et al.*, 2012a). Adding As^{III} to the culture in the wild type cell did not change *pstS2*::*lacZ* reporter activity during the PSR (∼900 MU), whereas reporter activity for all other genes was greatly enhanced (Fig. 2B). By contrast, all reporters were essentially silent in the Pi-stressed Δ*phoR* mutant (Fig. 2C) and induction of *pstS1*::*lacZ* and *phoB1*::*lacZ* were greatly attenuated in As^{III}-exposed Δ*phoR* cells relative to the wild type (compare Fig. 2B and D) (note *Y*-axis scale differences). In the Δ*aioS* mutant, all reporters likewise failed to induce except for extremely minor activity

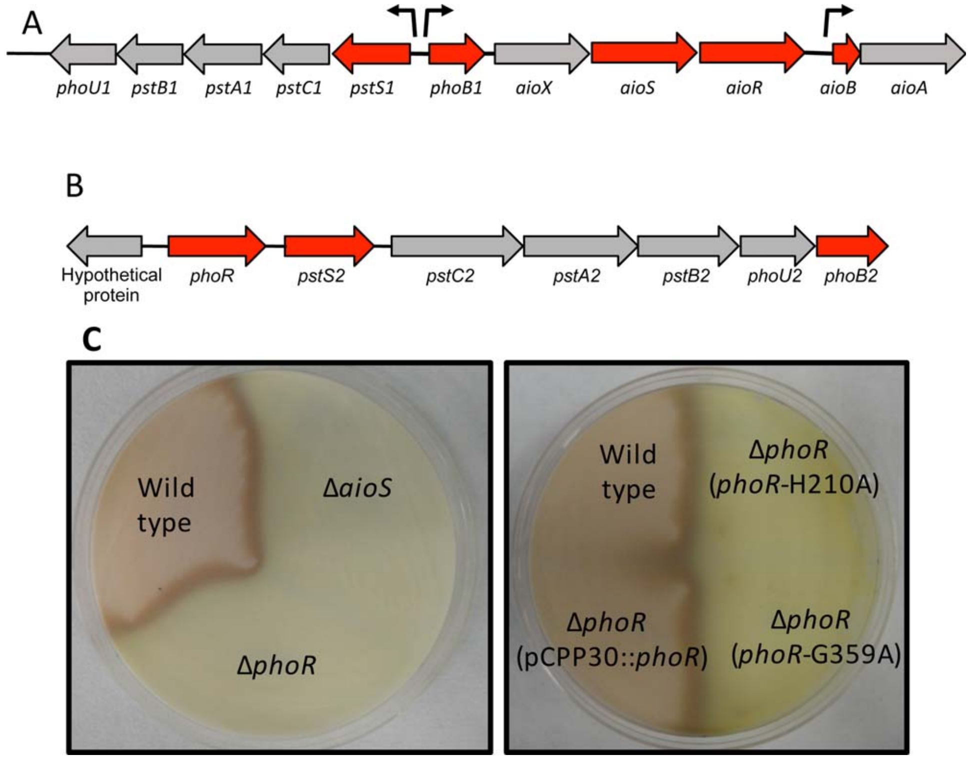

Fig. 1. *A. tumefaciens* strain 5A genome loci examined and qualitative analysis of As^{III} oxidation in the different mutants and recombinants.
A. Gene arrangement illustrating the position and proximity of the *aioSRBA* operon and adjacent *pho* and *pst* genes.
B. Operon arrangement of *pho* and *pst* genes located at a distal genome location relative to the *aio* operon. In both panels, genes highlighted in red represent genes mutated, or studied for expression or phosphorylation. Bent arrows indicate the approximate locations and transcriptional direction of promoters studied using *lacZ* fusion constructs.
C. $AgNO_3$ staining for As^{III} oxidation comparing wild type against the rescued Δ*phoR* mutant carrying the wild type *phoR* allele and the Δ*phoR* mutant carrying the *phoR* coding region with diagnostic amino acid substitutions. $MMNH_4$ agar plates (50 μM Pi and 1 mM As^{III}) were streak inoculated, incubated and flooded with 0.1 M $AgNO_3$ solution. Brown precipitate indicates the presence of As^{V} (positive As^{III} oxidation), while yellow indicates As^{III} (negative for As^{III} oxidation). [Colour figure can be viewed at wileyonlinelibrary.com]

exhibited by *phoB1*::*lacZ*. Apparent AioS regulatory control of *pstS1* and *pstS2* was completely unexpected because it implies reciprocal regulation of the PSR by the AioSR regulatory pair and thus a regulatory function separate from direct control of the arsenite oxidase structural genes. Importantly, *aioB*::*lacZ* in the wild type strain induced as expected (Kang *et al.*, 2012a), but failed to induce in either the Δ*phoR* mutant or the Δ*aioS* mutant, regardless of Pi or As^{III} levels (Fig. 2C–F). As viewed together, these reporter experiments demonstrate that both sensor kinases are essential for expression of the As^{III} oxidase genes (*aioBA*) as well as important elements of the PSR (*pst* and *pho* genes).

We next tested for reciprocal regulation and the relative importance of PhoR, AioS, Pi and As^{III} for influencing the PSR as measured by AP activity. In the absence of As^{III}, AP activity increased by approximately eightfold in Pi limited wild type as well as in the Δ*aioS* mutant and the Δ*pstS1* mutant (Fig. 3). Based on extensive work with *Escherichia coli* (Wanner, 1996), it would be predicted that AP would not induce in a Δ*phoR* mutant, which is what was observed (Fig. 3). However, as with the As^{III} oxidation phenotype discussed above, complementation of the Δ*phoR* mutant with the wild type *phoR* gene (pCPP30::*phoR*) returned this mutant to wild type status (Fig. 3). Based on the same rationale, it would also be predicted that AP would be over expressed in a *pstS* mutant; however, this differed between the Δ*pstS* mutants (Fig. 3). The Δ*pstS1* mutation had little effect on AP activity in the absence of As^{III}, but significantly so in As^{III} exposed cells (Fig. 3), suggesting that AioS somehow is involved in constraining the PSR, at least as assessed by AP activity. For the Δ*pstS2* mutant, AP overexpression was observed in both $+As^{III}$ and $–As^{III}$ cells (Fig. 3).

Signal transduction and regulatory cross-talk

Given the evidence implicating PhoR in regulating As^{III} oxidation as well as an As^{III} effect on some *pst*/*pho* genes (Fig. 2), we sought to establish whether the mechanism

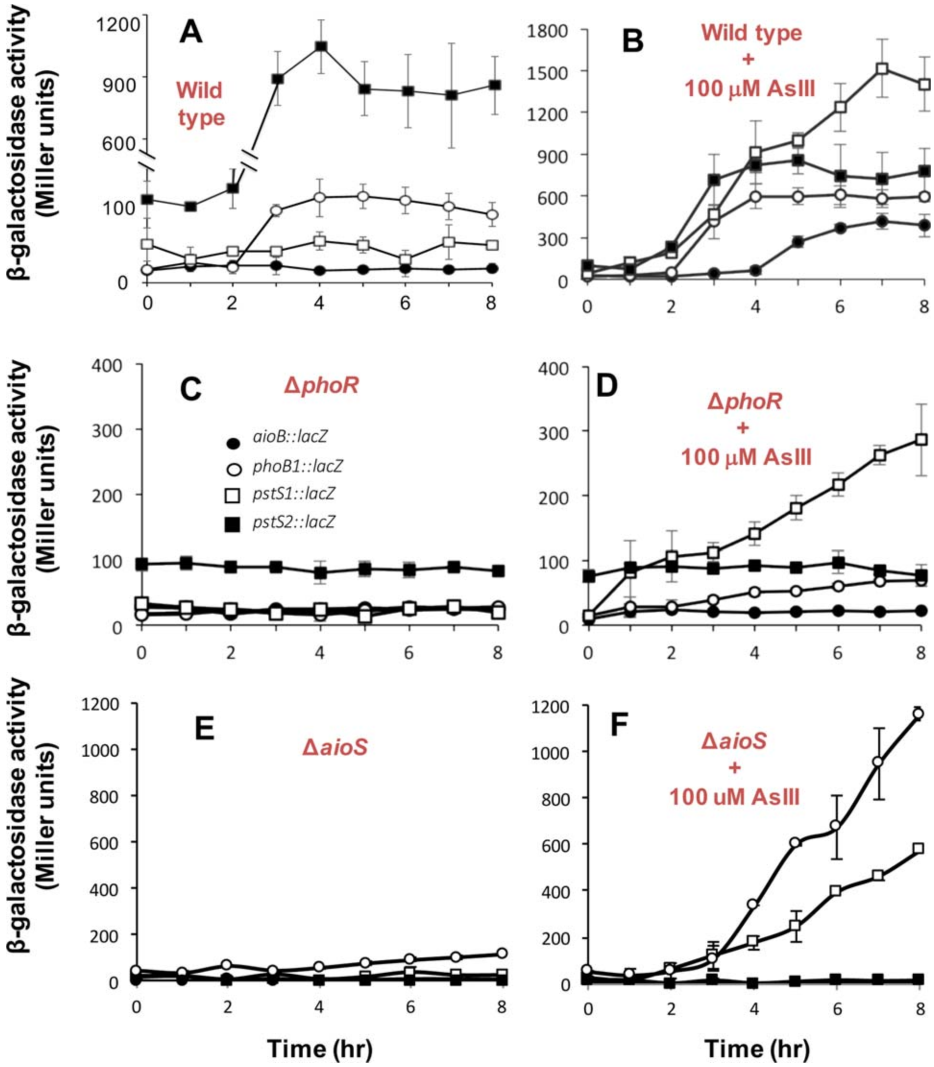

Fig. 2. A comparison of induction characteristics of *aioB, phoB1, pstS1 and pstS2* in the wild type strain 5A and the Δ*phoR* mutant. For all reporter genes, induction assays were in $MMNH_4$ (50 μM Pi). As^{III} (100 μM) was present or absent as indicated. Where visible, the error bars represent ± 1 SD. Note *Y*-axis scale differences for all panels accommodated expression levels for the most active reporters but visually suppressed that of some genes (e.g., *phoB1* in panels A and D). [Colour figure can be viewed at wileyonlinelibrary.com]

might possibly be linked to regulatory cross-talk wherein PhoR may phosphorylate AioR and or AioS may phosphorylate PhoB. The Phos-tag™ SDS-PAGE system can be used to electrophoretically separate the phosphorylated protein isoform from its non-phosphorylate counterpart (Kinoshita *et al.*, 2006), and was used here to qualitatively assess phosphotransfer within and between the regulatory pairs PhoBR and AioSR, using his-tag purified proteins (Supporting Information Fig. S2). In the presence of ATP (2 mM), autophosphorylation of PhoR and AioS occurred within one minute and was apparently quantitative after 20 min (Supporting Information Fig. S3). In experiments pairing PhoR plus ATP and AioS plus ATP with the response regulators AioR, PhoB1 or PhoB2 (Fig. 4), phosphorylation of all three response regulator proteins occurred. Mobility shifts of both the donor (PhoR or AioS) and receiver proteins (PhoB1, PhoB2, AioR) corresponded to non-phosphorylated and phosphorylated versions of each respectively (Fig. 4), but there was no visual evidence of these response regulator proteins autophosphorylating in the presence of ATP alone (lane C in Fig. 4). These experiments established evidence that these two-component systems are capable of communicating with one another and thus consistent with the dual PSR and As^{III} influences observed with the reporters.

As^V is beneficial to growth under PSR conditions

When considered together, results from the above experiments implied the biosynthesis of As^V, a Pi analogue, constitutes part of the bacterial PSR. If so, there could be a reasonable level of expectation that As^V may be of some benefit to the cell under PSR conditions. Culturing experiments using strains 5A and GW4 were initiated in nitric and hydrochloric acid washed flasks (to remove traces of Pi) and with media having As^V:Pi ratios of 10:1 so as to intentionally favor the bioavailability of As^V throughout and to effectively dispense with the need for As^{III} being first

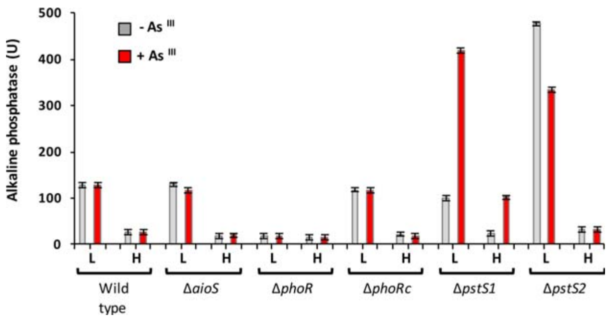

Fig. 3. Alkaline phosphatase activity in wild type and various mutants as a function of low (L) or high (H) Pi and with or without 100 μM As^{III}. Each result represents the mean value ± range from at least two replicate cultures and are representative assays. [Colour figure can be viewed at wileyonlinelibrary.com]

oxidized to As^V. Different levels of As^V employed reflect the tolerance levels of strains GW4 and 5A, while still allowing for reasonable growth rates and yields. Both strains exhibited extended growth when provided As^V (~39% and 17% increase in colony-forming counts for GW4 and 5A respectively) and growth corresponded to decreasing As^V levels in the culture fluids (Fig. 5A and B). When cultured under replete Pi conditions, the addition of As^V has no measureable effect (results not shown).

Potential Pi contamination in the As^V stock solution was also examined to determine if the enhanced growth resulted from contaminate Pi. Given the Pi detection limit of the ICP-MS instrumentation used, the As^V solution could account for a maximum Pi contamination of 0.10 ± 0.006 μM, amounting to at most a 0.01% increase in starting Pi levels. Follow-up experiments were conducted with a 10% increase in starting Pi levels (intentional to mimic a truly gross contamination scenario), yet no increase in stationary phase colony counts was observed (results not shown). This served to confirm that the increased growth observed with the addition of As^V did not result from Pi contamination of the As^V stock solution (or other media components) used in these experiments. Rather, extended growth was the result of the As^V amendment.

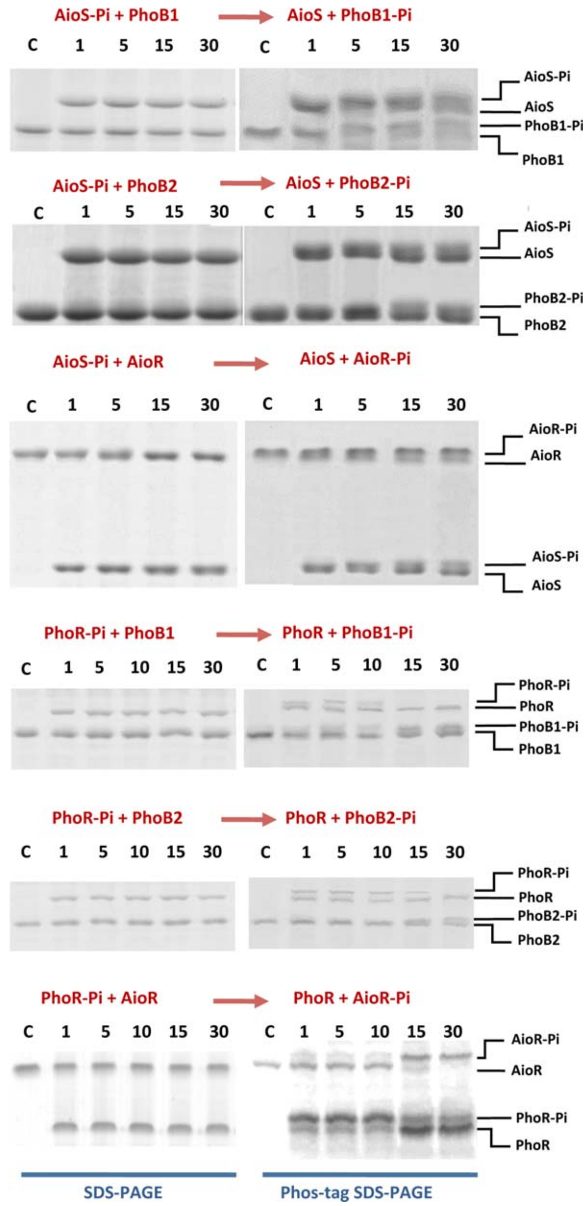

Fig. 4. In vitro phosphorelay reactions involving AioS and PhoR. Each sensor kinase was paired with PhoB1, PhoB2 and AioR to assess potential kinase activity. For each reaction, SDS-PAGE gels are on the left and the corresponding Phos-tag SDS-PAGE gels are shown on the right. Reaction times (minutes) are shown above each panel. 'C' lane corresponds to 30 minute reactions containing all components except the sensor kinases AioS or PhoR. [Colour figure can be viewed at wileyonlinelibrary.com]

Arsenic incorporation into cell materials

Given the documentation of arsenolipids and how microorganisms can alter cell wall/membrane components in response to Pi starvation (discussed below), we assessed the extent to which As^V may be incorporated into total cell biomass and more specifically, lipids. Cells of both strains were harvested at 32 h in experiments repeating those illustrated in Fig. 5A and B, and analyzed for As and Pi. Arsenic accumulation in GW4 was roughly 18-fold and 54-fold greater than in 5A (Fig. 5C) for total and lipid arsenic respectively. For both strains, minute levels of As were found in the –As^V control cultures (40- to 1200-fold less than +As^V cells, depending on the fraction examined), that we ascribe to carry-over from the starter culture (see *Experimental procedures*). Of the As accumulated in GW4, roughly 40% was allocated into lipids as compared to ~13% for 5A (Fig. 5D). Of particular interest, Pi was below detection in lipid extracts from As^V-treated GW4 and was depleted in As^V-treated 5A lipids (Fig. 5D), implying As^V competed against Pi for uptake and cellular

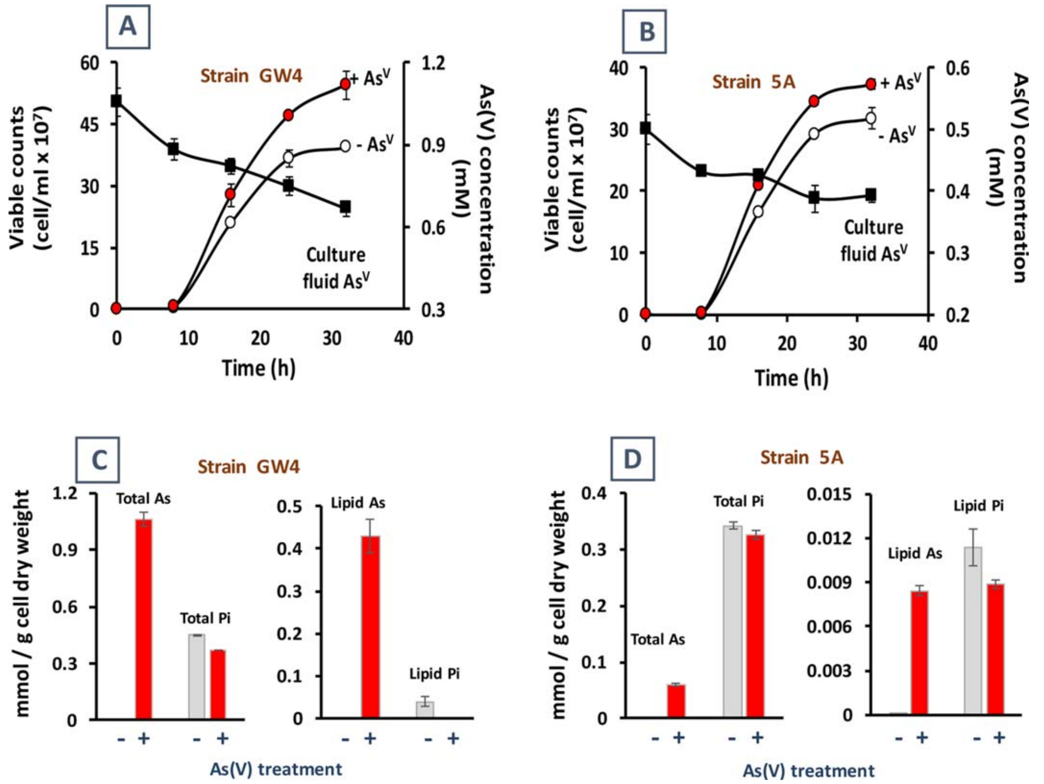

Fig. 5. Influence and fate of As^V added to Pi limited cultures of *A. tumefaciens* strains GW4 and 5A. (A, B) Growth enhancement and (C, D) cellular accumulation and allocation of As and Pi. At $t = 0$, the As:Pi ratio in the culture media was 10:1 for both strains. Data points and bar graphs represent the average ± standard error ($n = 3$) and are representative of numerous reproducible experiments for both strains. [Colour figure can be viewed at wileyonlinelibrary.com]

incorporation. Though quantitatively differing between strains, patterns of accumulation were similar; i.e., for both total and lipid assays, As accumulation coincided with decreased Pi. Indeed, Pi was consistently below detection in lipid fractions from As^V-treated GW4 (Fig. 5B). Arsenic levels and distribution in GW4 agree quite well with prior work with this strain (Wang *et al.*, 2015).

Discussion

Prior studies revealed how AioXSR are essential for induction of As^{III} oxidation (Kashyap *et al.*, 2006; Cai *et al.*, 2009; Sardiwal *et al.*, 2010; Liu *et al.*, 2012). These proteins are expressed in response to cell exposure to As^{III} and require PSR conditions, illustrating a relationship between Pi and As metabolisms (Kang *et al.*, 2012a; Wang *et al.*, 2015). The present study now describes the regulatory and mechanistic basis for this relationship and how co-induction of AP and *aioBA* is not a mere coincidence. PhoB, PhoU and PstS are all well known to be critical elements of the bacterial PSR (Hsieh and Wanner, 2010), which is global in a functional context (Van Bogelen *et al.*, 1996; Krol and Becker, 2004). Loss of these proteins in *A. tumefaciens* results in either complete loss or severely disrupted induction of *aioBA* and *aioSR* (Kang *et al.*, 2012a). Since PhoR is the sensor kinase that controls the PSR, we hypothesized it to be a control mechanism for As^{III} oxidation and thus was a focus of the current study.

Deletion of PhoR or mutational replacement of key PhoR amino acids (Fig. 1B, Supporting Information Fig. S1) known to be specifically involved in signal transduction established that canonical sensing and signalling is the transduction pathway controlling the induction of As^{III} oxidation. In combination with our prior efforts that documented integration of As^{III} oxidation and Pi metabolism (Kang *et al.*, 2012a; Wang *et al.*, 2015), this provides strong evidence in support of a new model (Fig. 6) wherein under conditions of low Pi and the presence of As^{III}: (i) As^{III} enters the cell via an aquaglycerol porin and interacts with all ArsRs and in this specific case ArsR1 to release from its DNA binding sites, and thereby opening the promoter regions of *pstS1* and *phoB1* (purple vectors); (ii) PhoR-Pi phosphorylates its cognate regulator PhoB (PhoB1 or PhoB2) as is conventionally viewed for the PSR (Wanner, 1996; Hsieh and Wanner, 2010); (iii) PhoB-Pi then activates transcription of *aioXSR* via a Pho box (PhoB binding sequence associated with *aioX*, 33 bp upstream of the *aioX* translational start site) (Hsieh and Wanner, 2010); (iv) the resulting AioX, AioS and AioR are then in place to

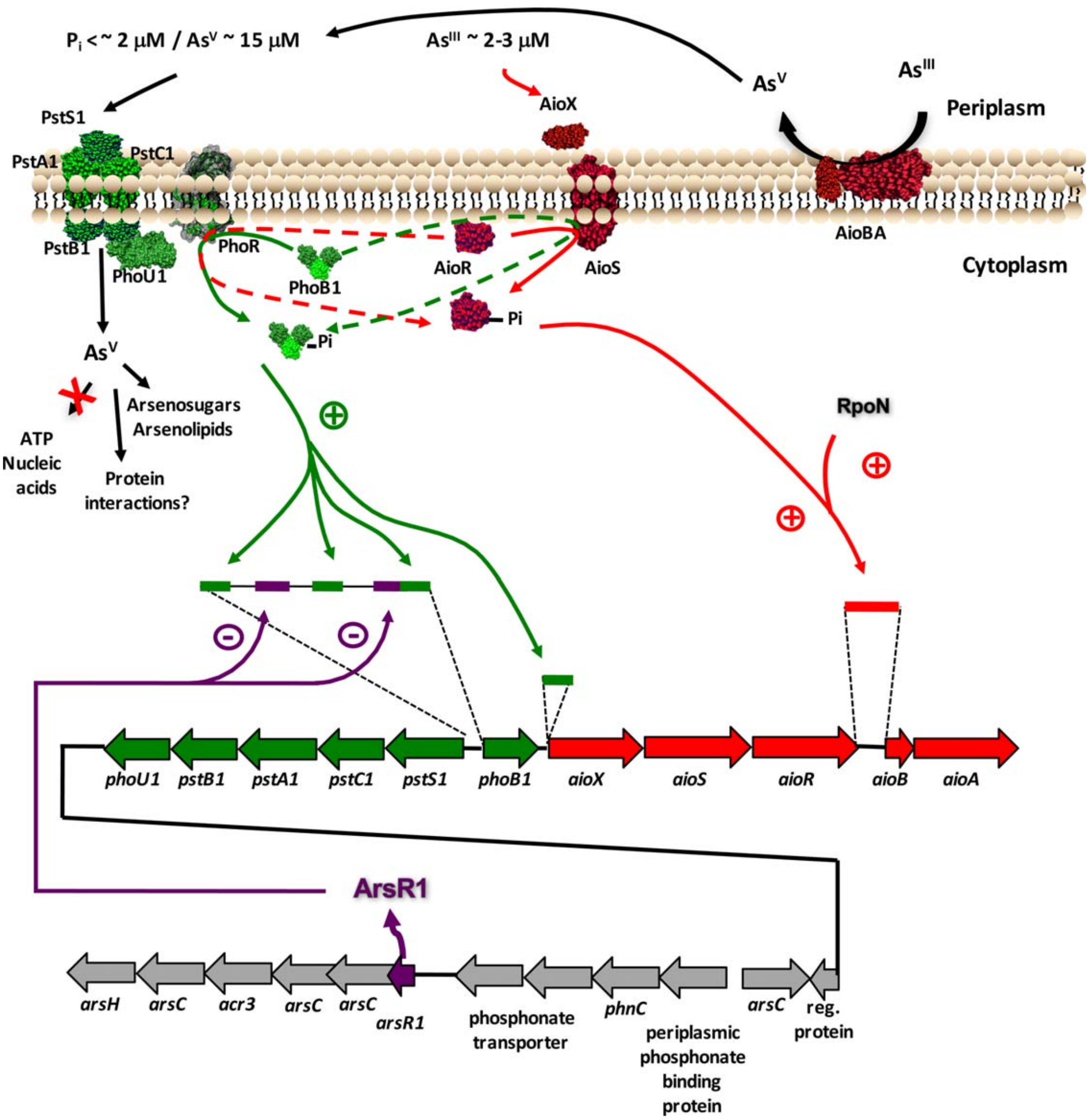

Fig. 6. New model depicting the integration of As^{III} oxidation into the PSR in *A. tumefaciens*. Under conditions where As^{III} is present and environmental Pi is depleted, As^{III} enters the cell via an aquaglycerol porin (not shown) and interacts with ArsR to cause ArsR to release and thereby opens the promoter regions of *pstS1* and *phoB1* (purple vectors). The PSR signal is transduced via PhoR to the transcriptional activator PhoB1 (green vectors), resulting in the full induction of *phoB1* and *pstS1*. PhoB1 then activates expression of *aioXSR*. As^{III} is bound by the periplasmic AioX, which interacts with AioS to initiate the As^{III} signal transduction to the transcriptional activator AioR (red vector arrows). Phosphorylated AioR then activates transcription of *aioBA* in association with RpoN. The resulting As^{III} oxidation generates As^V, which is then taken up and can be utilized for sparing Pi for redistribution for critical cellular components (e.g., nucleic acids) or for essential cell functions (e.g., ATP metabolism). Dashed arrows depict cross-talk between AioS and PhoB1/PhoB2 and between PhoR and AioR. [Colour figure can be viewed at wileyonlinelibrary.com]

accept and transduce the As^{III} signal, resulting in AioR-Pi initiating transcription of *aioBA* in conjunction with the transcriptional activator RpoN (Koechler *et al*., 2010; Kang *et al*., 2012b). The *in vitro* phosphorylation data (Fig. 4) provides evidence of how this PhoR-dependent mechanism could also include a regulatory cross-talk scenario whereby PhoR phosphorylates AioR as well as AioS phosphorylating PhoB1/2, each of which could serve to strengthen/reinforce both response circuitries. Cross-talk based phosphorylation of PhoB in *E. coli* is well documented (Wanner, 1996; Hsieh and Wanner, 2010).

Other evidence strongly argues for regulatory inter-relatedness and reciprocity. AP activity is greatly enhanced by As^{III} in both *pstS* mutants relative to wild type, although an alternative interpretation may be that As^{III} actually decreases AP in the $\triangle$*pstS2* mutant relative to the already high constitutive activity in the absence of As^{III} (Fig. 3). The PstSCAB complex is known to have a deactivating regulatory role, turning off the PSR (Wanner, 1996; Hsieh and Wanner, 2010) and thus in the $\triangle$*pstS* mutants the PSR modulating mechanism is no longer active, resulting in greatly enhanced AP (Fig. 3). However, this effect is As^{III}

dependent for PstS1. We have previously shown that As^{III} induces *pstS1* transcription via ArsR1 de-repression (Kang *et al*., 2012a). The resulting PstS1 could potentially function to modulate the PSR and thus constraining AP activity. Our prior work with PstS1 failed to detect As^{III} binding, but did find evidence of As^{V} binding ($K_D \sim 15$ μM) (Wang *et al*., 2015). Presumably this is the first step to facilitate As^{V} uptake via the PstCAB transporter (normally thought to be the high affinity Pi transporter), perhaps serving to load the PstSCAB complex so as to mimic adequate Pi and thus quench the PSR while acquiring a Pi replacement. One of the biggest surprises deriving from this study was the complete lack of induction of the *pstS1* or *pstS2* reporters in the Δ*aioS* mutant (Fig. 2), indicating the depth of how the PSR and the AioSR regulatory systems are linked.

Microarray analysis of *Herminiimonas* also shows *aioBA* induction coinciding with *pho* and *pst* expression as part of a transcriptional response to As^{III} (Cleiss-Arnold *et al*., 2010). We suggest the delayed induction of the *aio* genes in *Herminiimonas* derives from the same PSR-related regulation and induction as we have described (Kang *et al*., 2012a and herein). Initial culture Pi levels used for the *Herminiimonas* work ('CDM' medium ∼57 μM, as originally described in Muller *et al*., 2003) would initially inhibit *aioBA* expression; however, with incubation and cellular Pi uptake over only a few hours, the culture would transition to a PSR situation ('late response' as described, Cleiss-Arnold *et al*., 2010) and thus enabling *aio* induction. Studies with *Pseudomonas xanthomarina* S11 that lacks recognizable *aioXSR* genes led Koechler *et al.* (2015) to conclude that *aioBA* expression was constitutive in this bacterium. However, these experiments also used CDM medium and gene expression was assayed after 24 h, a period in which the cells would have reduced or indeed exhausted media Pi, leading to the induction of the PSR and the *aio* genes. Of particular importance in this regard, other As^{III} oxidizing microorganisms lack the *aioXSR* genes (Chen *et al*., 2015), clearly implying some other regulatory system is in place. For example, As^{III} oxidation in *Halomonas* sp. HAL-1 is controlled by PhoRB in low Pi media, although apparently by some other regulatory system when the cells are grown in high Pi media (Chen *et al*., 2015). Regardless of Pi level however, As^{III} is required for *aioBA* induction in HAL-1 under all conditions, demonstrating the constant regulatory linkage between As^{III} and *aioBA* expression. At present, we suggest that PhoRB is involved or indeed essential for regulating As^{III} oxidation in many if not all microorganisms that do so. The requirement of AioXSR is not universal and perhaps reflects a later evolutionary modification (Alm *et al*., 2006) of a PhoRB-only control regime.

As^{V} incorporation into Pi-limited cells (Fig. 5) is consistent with recent studies documenting arsenic bioaccumulation in various bacteria (Takeuchi *et al*., 2007; Yan *et al*., 2014; Pandey and Bhatt, 2015; Wang *et al*., 2015). Further, As^{V} enhanced growth under PSR conditions is consistent with the growth data published by Wolfe-Simon *et al.* (2011) and thus consistent with their hypothesis. However, we draw distinctions that significantly constrain that hypothesis. As currently understood, arsenic incorporation into biomass should not involve arsenate esters in key structures (e.g., nucleic acids or ATP metabolism) because the bond is viewed to be too unstable (Rosen *et al*., 2011). However, we draw attention to a recent study by the Rosen group that examined the functional importance of a gene encoding a glyceraldehyde-3-phosphate dehydrogenase (GAPDH) that is found in many *ars* operons and up-regulated in response to arsenic exposure (Chen *et al*., 2016). The GAPDH was shown to incorporate arsenate into glyceraldehyde-3-phosphate, generating 1-arseno-3-phosphoglycerate that is an export transport substrate for ArsJ. Chen *et al.* (2016) regard it as an arsenate-specific resistance mechanism, but nevertheless illustrates how arsenate esters may exhibit sufficient stability so as to participate in metabolism in a measurable way and perform in a manner consistent with expectations – in this context, arsenic resistance.

The C-As bond is quite stable. The specific biochemical pathway(s) involved remain to be identified, although at present it appears that arsenic methylation (via ArsM) (Yang and Rosen, 2016) is an essential first step because methylated pentavalent arsenicals are typically a feature of As-C containing carbon compounds such as arsenosugars and arsenolipids (Dembitsky and Levitsky, 2004). Cellular localization of As in our *A. tumefaciens* strains shows incorporation into lipids (Fig. 5C and D and Wang *et al*., 2015), suggesting some type of arsenolipid moiety, which are well documented and naturally occurring in marine animals (Dembitsky and Levitsky, 2004) and macroalgae (Francesconi and Kuehnelt, 2002; Francesconi, 2010; Garcia-Salgado *et al*., 2012; Raab *et al*., 2013), which provides ample precedent for As^{V} incorporation into specific cellular structures. Beyond the lipid fraction (Fig. 5), approximately half of the As^{V} in 5A and GW4 cannot be accounted for in this study. Protein interactions with both trivalent and pentavalent arsenicals have been documented, and thus offer potential explanations for the non-lipid arsenic in our study [reviewed by Shen *et al.* (2013)]. We have previously observed significant As^{V} co-purifying with protein extract fractions of strain GW4 (Wang *et al.* 2015), and thus we predict that other localizations likely include some type of protein interaction. Our current efforts are targeting this issue.

Under PSR conditions, different bacteria have been shown to replace up to 40% of cellular Pi by: (i) recycling phospholipids (Geiger *et al*., 1999; López-Lara *et al*., 2005); (ii) down-regulating genes encoding

Table 1. Bacterial strains, plasmids and primers used in this study.

Strain or plasmid	Relevant markers and characteristics	Reference or
Plasmid		
pLSP-KT2lacZ	KmR, *oriV*, *lacZ* -fusion vector used for *lacZ* fusion	Kang *et al.* (2012a)
pLSP-KT2lacZ:: *aioB ::lacZ*)	pLSP-KT2lacZ carrying the *aioB* promoter fused to	Kang *et al.* (2012a)
pLSP-	pLSP-KT2lacZ carrying the *phoB1* promoter fused to	Kang *et al.* (2012a)
pLSP-	pLSP-KT2lacZ carrying the *pstS1* promoter fused to	Kang *et al.* (2012a)
pLSP-	pLSP-KT2lacZ carrying the *pstS2* promoter fused to	This study
pJQ200sk	Gen ^{R} , *traJ*, *oriT*, *sacB* , suicide vector to introduce	Kang *et al.* (2012a)
pJQ200sk- *phoR*	pJQ200sk vectoring *phoR* -deleted region	This study
pJQ200sk- *aioS*	pJQ200sk vectoring *aioS* -deleted region	This study
pCPP30	TcR, Tra- Mob+ IncP replicon, broad host range	Kang *et al.* (2012a)
pCPP30:: *phoR*	pCPP30 carrying the wild type phoR for complementation of 5A (Δ *phoR*) mutant	This study
pCPP30:: *phoR*- H21A	pCPP30 carrying the H21A amino acid substitution in	This study
pCPP30:: *phoR*- G359A	pCPP30 carrying the G359A amino acid substitution	This study
pET-28a(+)	Protein expression vector for protein purification	Novagen
pProEXHTa	Protein expression vector for protein purification	Novagen
Strain (reporter constructs):		
Agrobacterium		
5A	Wild type, soil isolate, As(III) oxidizing	Lab stock
GW4	Wild type, soil isolate, As(III) oxidizing	Lab stock
5A (*aioB ::lacZ)*	Km ^{R} , 5A carrying pLSP-P containing *lacZ* fused to the *aioB* promoter	Kang *et al.* (2012a)
5A (*phoB1 ::lacZ*)	Km ^{R} , 5A carrying pLSP-P containing *lacZ* fused to the *phoB1* promoter	Kang *et al.* (2012a)
5A *(pstS1 ::lacZ)*	Km ^{R} , 5A carrying pLSP-P containing *lacZ* fused to the *pstS1* promoter	Kang *et al.* (2012a)
5A(pstS2 ::lacZ)	Km ^{R} , 5A carrying pLSP-P containing *lacZ* fused to the *pstS2* promoter	This study
5A (Δ *phoR)*	Strain 5A containng a deletion mutation in *phoR*	This study
5A (Δ *phoR, aioB::lacZ)*	Strain 5A *aioS* mutant carrying the *aioB::lacZ*	This study
5A (ΔphoR, *phoB1 ::lacZ)*	Strain 5A *aioS* mutant carrying the *phoBl::lacZ*	This study
5A (ΔphoR, *pstS1 ::lacZ*)	Strain 5A *aioS* mutant carrying the *pstS1::lacZ*	This study
5A (ΔphoR, *pstS2 ::lacZ*)	Strain 5A *aioS* mutant carrying the *pstS2::lacZ*	This study
5A (Δ *aioS)*	Strain 5A containng a deletion mutation in *aioS*	This study
5A (Δ *aioS, aioB::lacZ)*	Strain 5A *aioS* mutant carrying the *aioB::lacZ*	This study
5A (Δ *aioS* , *phoB1 ::lacZ*)	Strain 5A *aioS* mutant carrying the *phoB1::lacZ*	This study
5A (Δ *aioS* , *pstS1 ::lacZ*)	Strain 5A *aioS* mutant carrying the *pstS1::lacZ*	This study
5A (Δ *aioS* , *pstS2 ::lacZ*)	Strain 5A *aioS* mutant carrying the *pstS2::lacZ*	This study
Escherichia coli		
S17-1	Pro - Mob $^{+}$; conjugation donor	Lab stock
BL21 (DE3)	(Cam ^{R})	Invitrogen

synthesis of Pi-rich techoic acids (Lang *et al.*, 1982; Salzberg *et al.*, 2015) and (iii) synthesizing sulfolipids (Guler *et al.*, 1996; Souza *et al.*, 2008; Zavaleta-Pastor *et al.*, 2010). Arsenolipid replacement of phospholipids under PSR conditions could function analogously, sparing Pi to be recycled for maintenance of critical biomolecules wherein Pi is not replaceable by As^{V}. In this context, we draw attention to the fact that the lipid fraction in As^{V}-treated cells was enriched with As, but reduced in P (strain 5A, Fig. 5D) or undetectable (strain GW4, Fig. 5C). Merchant and Helmann (2012) concluded that '. . .there is not a single documented example of As replacing P in a biological molecule that retains its normal function in the cell' and that '. . . replacement of a significant amount of P by As is chemically implausible'. We suggest this issue is worthy of additional scrutiny.

Experimental procedures

Bacterial strains and growth conditions

The bacterial strains and plasmids used in this study are detailed in Table 1, and PCR primer sequences used are provided in Supporting Information Table S1. The *A. tumefaciens* strains were cultured at 30°C in a defined minimal mannitol medium ($MMNH_4$) (Somerville and Kahn, 1983) containing mannitol as a carbon and energy source with aeration by shaking. *Escherichia coli* strains Top10 and S17-1 were grown at 37°C in Lysogeny broth (LB) medium. Bacterial growth was monitored via measurements of culture optical density using a SpectraMax microtiter plate reader (Molecular Devices, California) or via viable plate counts, depending on the experimental requirements. For experiments examining the influence of As^{V} on growth of Pi stressed *A. tumefaciens* cultures, the liquid $MMNH_4$ media was modified to contain an As^{V}:Pi ratio of 10:1; 1 mM As^{V}:0.1 mM Pi for strain GW4 or 0.5 mM As^{V}:0.05 mM Pi for strain 5A. Culture growth in these experiments was determined by viable plate counts on $MMNH_4$ agar.

Plasmid isolation, gel electrophoresis, transformation and PCR amplification of DNA were conducted as described previously (Kang *et al.*, 2012a,b). When required, the $MMNH_4$ medium was supplemented with 100 $\mu g\ ml^{-1}$ kanamycin (Km) for pLSP selection and maintenance, 80 $\mu g\ ml^{-1}$ gentamycin (Gen), 20 $\mu g\ ml^{-1}$ tetracycline (Tc), or 15% sucrose for the pJQ200SK selection. *E. coli* was grown with 50 $\mu g\ ml^{-1}$ Km, 20 $\mu g\ ml^{-1}$ Gen, 20 $\mu g\ ml^{-1}$ Tc. Gene deletion and amino acid replacement mutations were constructed using techniques we have previously described (Liu *et al.*, 2012). The various plasmid constructs carrying the different mutated genes were transformed into *E. coli* S17-1 and mobilized to *A. tumefaciens* 5A by biparental-conjugation. Levansucrase selection was use for isolation of deletion mutants as previously described (Kang *et al.*, 2012a,b). Reporter gene constructs used plasmid pLSP-KT2lacZ as described in our prior studies (Kang *et al.*, 2012a,b).

Protein expression and purification

The expression plasmid pET-28a(+) (Novagen) was used to express and synthesize PhoR, PhoB1, PhoB2 and AioS, while pProEXHTa (Novagen) was used to express AioR. The *phoR* coding sequence without the N-terminal membrane spanning region (nucleotides 319–1269 bp) was amplified using PhoR-F and PhoR-R primers (Supporting Information Table S1) and cloned into *Bam*HI-*Eco*RI digested sites of pET-28a(+), resulting in pET-PhoR with a N-terminal His tag. Likewise, the *aioS* N-terminal coding sequence without the membrane-spanning region (nucleotides 582–1464 bp) was amplified using AioS-F and AioS-R (Supporting Information Table 1). The PCR product was digested with *Bam*HI and *Not*I, and cloned into pET-28a(+), yielding pET-AioS with the His tag in both N-terminal and C-terminals (enhanced binding to resin). The complete coding regions of *phoB1* and *phoB2* were PCR-cloned into pET-28a(+), resulting in plasmids pET-PhoB1 and pET-PhoB2, both with an N-terminal His tag. Similarly, the complete coding region of *aioR* was PCR cloned into pProEXHTa, which allowed for enhanced heterologous AioR expression and purification with an N-terminal His tag. All of the plasmids were transformed into *E. coli* BL21 Star^{TM} (DE3) pLysS (Invitrogen) for expression.

Heterologous protein expression and purification

Expression of PhoR, PhoB1 and PhoB2 were induced by the addition of 0.5 mM IPTG when the optical density of cultures reached 0.4 at 600 nm. Cultures were incubated a further 4-h with shaking at 28°C. Expression of AioS and AioR was induced with 0.2 and 0.02 mM IPTG respectively, when culture optical density (600 nm) was less than 0.1. Cultures were further incubated for 8 and 12 h at 20°C respectively. After induction, all proteins were purified via the following procedure. Cells were harvested by centrifugation (13 400*g* for 5 min at 4°C), washed twice with 50 mM Tris-HCl (pH 8.0) and then the bacterial cells were resuspended with 10 ml 50 mmol l^{-1} Tris-HCl containing 1 μM phenylmethanesulfonyl fluoride and lysed at 4°C (Ultrahigh pressure continuous flow cell disruptor JN-3000PLUS, JNBIO). Unbroken cells were removed by centrifugation (8400 $\times$ *g* for 5 min), with the supernatant then mixed with 1 ml pre-equilibrated ProfinityTM IMAC Resins (Bio-RAD) and gently agitated on ice for 1 h. Loaded resins were then transferred into a 10 ml gravity-flow column, and washed with 5 ml Tris-HCl, 40 mM imidazole. The protein was eluted in 2 ml Tris-HCl with 300 mmol l^{-1} imidazole (Liu *et al.*, 2012). Protein quantity and quality was assessed spectrophotometrically (NanoDrop 2000, Thermo) and SDS-PAGE.

Phosphorylation assays

The Phos-tag system (Kinoshita *et al.*, 2006) was used to identify changes in phosphorylation state of the different proteins. Autophosphorylation of the sensor kinases PhoR (4 μM) and AioS (6 μM) was carried out in a 200 μl reaction buffer containing 50 mM Tris-HCl (pH 8.0), 50 mM KCl, 10 mM $MgCl_2$ and 2 mM ATP. After incubating for 1, 5, 10, 15 and 20 min, 40 μl of the reaction mixture was transferred to 10 μl stop buffer containing 5 mM Tris-HCl (pH6.5), 1% w/v SDS, 10% v/v glycerol, 5% v/v 2-sulfanylethanol and 0.03% w/v bromophenol blue (BPB).

For trans-phosphorylation reactions involving PhoR, the 200 μl reactions contained 4 μM PhoR and 6 μM of AioR, PhoB1 or PhoB2. For trans-phosphorylation reactions involving AioS and response regulators PhoB1, PhoB2 and AioR, the 200 μl reaction mixes included 6 μM each of AioS, PhoB1, PhoB2 or AioR. For both sets of reactions, samples were removed after 1, 5, 10, 15 and 30 min incubation and treated as described above. Samples were then examined in SDS-PAGE gels with or without the addition of 50 mM Phos-tag and 100 mM $MnCl_2$, according to manufacturer's protocol (Wako Pure Chemical Industries). Gel mobility of the phosphorylated and non-phosphorylated proteins was visualized in SDS-PAGE and Phos-tag^{TM} SDS-PAGE.

As^V bioaccumulation

Agrobacterium tumefaciens strains were pre-cultured at 30°C in $MMNH_4$ containing 1.0 mM As^{III} or 500 μM As^{III} for GW4 and 5A respectively. Cells were washed 3X with Tris-HCl (pH = 7.2) and suspended into 5 ml Tris-HCl (pH = 7.2), and then used to inoculate 100 ml $MMNH_4$ cultures at a starting OD_{600} of 0.05. Strain 5A cultures contained 50 μM Pi with or without 500 μM As^V, whereas strain GW4 contained 0.1 mM Pi, with or without 1 mM As^V. After 32 h cultivation, 20 ml cultures were harvested for arsenic analysis. For total arsenic, cells were collected by centrifugation (13 400 g for 5 min at 4°C), washed 3X with 0.85% NaCl, resuspended in 0.5 ml concentrated HNO_3, digested at 100°C and then diluted 10-fold to reduce the HNO_3 concentration to 10% for ICP-MS analysis. For lipid extracts, 100 ml cultures were collected by centrifugation, washed 3X with 0.85% NaCl and then resuspended into 0.45 ml ice cold 100 mM Tris-HCl buffer (pH = 7.6). Two volumes of ice cold 1:2 chloroform:methanol was added and then samples vortexed vigorously, followed by adding 0.3 ml ice cold chloroform and vortexing for 30 s. Finally, cells were sonicated on ice for 10 s, centrifuged at 3000 g and then the organic layer (lower layer) was transferred into fresh glass vials, and further extracted with 0.5 ml ice cold chloroform. After vortexing (30 s), the organic layer was separated by centrifugation and removed, dried under a nitrogen stream at room temperature and resuspended in 5 ml 10% HNO_3. The Pi and As concentrations were analyzed via HPLC-ICP-MS and normalized by the cell dry weight.

To estimate As carryover from the pre-culture and/or from As in the medium that might co-extract, prior to harvesting cells in the $-As^V$ control cultures were heat killed to inhibit uptake, the medium was then spiked with the same starting As^V as in $+As^V$ cultures and then washed and extracted as above. Based on numerous trials, As carryover/bleed-through was typically undetectable, but otherwise account for a maximum 8.5% of As detected in the $+As^V$ treated cells. Consequently, this type of artifact was not considered a problem.

Acknowledgements

This research was supported by the U.S. National Science Foundation to T.R.M. and B.B. (MCB 0817170 and MCB 1413321), by the Montana Agricultural Experiment Station (911310) to T.R.M. and by the National Natural Science Foundation of China (31670108) to G.W. and (31500088) for Q.W.

The authors are not aware of any affiliations, memberships, funding or financial holdings that might be perceived as affecting the objectivity of this review and declare there is no conflict of interests.

References

Alm, E., Huang, K., and Arkin, A. (2006) The evolution of two-component systems in bacteria reveals different strategies for niche adaptation. *PLoS Comput Biol* **2:** e143.

Andres, J., and Bertin, P.N. (2016) The microbial genomics of arsenic. *FEMS Microbiol Revs* **40:** 299–322.

Cai, L., Liu, G., Rensing, C., and Wang, G. (2009) Genes involved in arsenic transformation and resistance associated with different levels of arsenic-contaminated soils. *BMC Microbiol* **9:** 4.

Chen, F., Cao, Y., Wei, S., Li, Y., Li, X., Wang, Q., and Wang, G. (2015) Regulation of arsenite oxidation by the phosphate two-component system PhoBR in *Halomonas* sp. HAL1. *Front Microbiol* **6:** 923.

Chen, J., Yoshinaga, M., Garbinski, L.D., and Rosen, B.P. (2016) Synergistic interaction of glyceraldehydes-3-phosphate dehydrogenase and ArsJ, a novel organoarsenical efflux permease, confers arsenate resistance. *Mol Microbiol* **100:** 945–953.

Cleiss-Arnold, J., Koechler, S., Proux, C., Fardeau, M.L., Dillies, M.A., Coppee, J.Y., *et al*. (2010) Temporal transcriptomic response during arsenic stress in *Herminiimonas arsenicoxydans*. *BMC Genomics* **11:** 709.

Dembitsky, V.M., and Levitsky, D.O. (2004) Arsenolipids. *Prog Lipid Res* **43:** 403–448.

diCenzo, G.C., Sharthiya, H., Nanda, A., Zamani, M., and Finan, T.M. (2017) PhoU allows rapid adaptation to high phosphate concentrations by modulating PstSCAB transport rate in *Sinorhizobium meliloti*. *J Bacteriol* **199:** e00143-17.

Francesconi, K.A., and Kuehnelt, D. (2002) Arsenic compounds in the environment. In: Fankenberger, W.T. (ed.). *Environmental Chemistry of Arsenic*, New York: Marcel Dekker. pp. 51–94.

Francesconi, K.A. (2010) Arsenic species in seafood: origin and human health implications. *Pure Appl Chem* **82:** 373–381.

Gao, R., and Stock, A.M. (2009) Biological insights from structures of two-component proteins. *Annu Rev Microbiol* **63:** 133–154.

Garcia-Salgado, S., Raber, G., Raml, R., Magnes, C., and Francesconi, K.A. (2012) Arsenosugar phospholipids and arsenic hydrocarbons in two species of brown macroalgae. *Environm Chem* **9:** 63–66.

Geiger, O., Röhrs, V., Weissenmayer, B., Finan, T.M., and Thomas-Oates, J.E. (1999) The regulator gene *phoB* mediates phosphate stress controlled synthesis of the membrane lipid diacylglyceryl-N,N,N-trimethylhomoserine in *Rhizobium* (*Sinorhizobium*) *meliloti*. *Mol Microbiol* **32:** 63–73.

Guler, S., Seeliger, A., Hartel, H., Renger, G., and Benning, C. (1996) A null mutant of *Synechococcus* sp. PCC7942 deficient in the sulfolipid sulfoquinovosyl diacylglycerol. *J Biol Chem* **271:** 7501–7507.

Hsieh, Y.J., and Wanner, B.L. (2010) Global regulation by the seven-component Pi signaling system. *Curr Opin Microbiol* **13:** 198–203.

Kang, Y.S., Heinemann, J., Bothner, B., Rensing, C., and McDermott, T.R. (2012a) Integrated co-regulation of bacterial arsenic and phosphorus metabolisms. *Environ Microbiol* **14:** 3097–3109.

Kang, Y.S., Bothner, B., Rensing, C., and McDermott, T.R. (2012b) Involvement of RpoN in regulating bacterial arsenite oxidation. *Appl Environ Microbiol* **78:** 5638–5645.

Kashyap, D.R., Botero, L.M., Franck, W.L., Hassett, D.J., and McDermott, T.R. (2006) Complex regulation of arsenite oxidation in *Agrobacterium tumefaciens*. *J Bacteriol* **188:** 1081–1088.

Kinoshita, E., Kinoshita-Kikuta, E., Takiyama, K., and Koike, T. (2006) Phosphate-binding tag, a new tool to visualize phosphorylated proteins. *Mol Cell Proteomics* **5:** 749–757.

Koechler, S., Arsène-Ploetze, F., Brochier-Armanet, C., Goulhen-Chollet, F., Heinrich-Salmeron, A., Jost, B., *et al*. (2015) Constitutive arsenite oxidase expression detected in arsenic-hypertolerant *Pseudomonas xanthomarina* S11. *Res Microbiol* **166:** 205–214.

Koechler, S., Cleiss-Arnold, J., Proux, C., Sismeiro, O., Dillies, M.A., Goulhen-Chollet, F., *et al*. (2010) Multiple controls affect arsenite oxidase gene expression in *Herminiimonas arsenicoxydans*. *BMC Microbiol* **10:** 53–65.

Krol, E., and Becker, A. (2004) Global transcriptional analysis of the phosphate starvation response in *Sinorhizobium meliloti* strains 1021 and 2011. *Mol Genet Genomics* **272:** 1–17.

Lang, W.K., Glassey, K., and Archibald, A.R. (1982) Influence of phosphate supply on teichoic acid and teichuronic acid content of *Bacillus subtilis* cell walls. *J Bacteriol* **151:** 367–375.

Liu, G., Liu, M., Kim, E.-H., Maaty, W.S., Bothner, B., Lei, B., *et al*. (2012) A periplasmic arsenite-binding protein involved in regulating arsenite oxidation. *Environ Microbiol* **14:** 1624–1634.

López-Lara, I.M., Gao, J.L., Soto, M.J., Solares-Pérez, A., Weissenmayer, B., Sohlenkamp, C., *et al*. (2005) Phosphorus-free membrane lipids of *Sinorhizobium meliloti* are not required for the symbiosis with alfalfa but contribute to increased cell yields under phosphorus-limiting conditions of growth. *Mol Plant Micro Interact* **18:** 973–982.

Merchant, S.S., and Helmann, J.D. (2012) Elemental economy: microbial strategies for optimizing growth in the face of nutrient limitation. *Adv Microb Physiol* **60:** 91–210.

Muller, D., Lièvremont, D., Simeonova, D.D., Hubert, J.C., and Lett, M.C. (2003) Arsenite oxidase *aox* genes from a metal-resistant beta-proteobacterium. *J Bacteriol* **185:** 135–141.

Murphy, J.N., and Saltikov, C.W. (2009) The ArsR repressor mediates arsenite-dependent regulation of arsenate respiration and detoxification operons of *Shewanella* sp. strain ANA-3. *J Bacteriol* **191:** 6722–6731.

Pandey, N., and Bhatt, R. (2015) Arsenic resistance and accumulation by two bacteria isolated from a natural arsenic contaminated site. *J Basic Microbiol* **55:** 1275–1286.

Raab, A., Newcombe, C., Pitton, D., Ebel, R., and Feldmann, J. (2013) Comprehensive analysis of lipophilic arsenic species in a brown Alga (Saccharina latissima). *Anal Chem* **85:** 2817–2824.

Rosen, B.P., Ajees, A.A., and McDermott, T.R. (2011) Life and death with arsenic. Arsenic life: an analysis of the recent report "A bacterium that can grow by using arsenic instead of phosphorus". *Bioessays* **33:** 350–357.

Salzberg, L.I., Botella, E., Hokamp, K., Antelmann, H., Maaß, S., Becher, D., *et al*. (2015) Genome-wide analysis of phosphorylated PhoP binding to chromosomal DNA reveals several novel features of the PhoPR-mediated phosphate limitation response in *Bacillus subtilis*. *J Bacteriol* **197:** 1492–1506.

Sardiwal, S., Santini, J.M., Osborne, T.H., and Djordjevic, S. (2010) Characterization of a two-component signal transduction system that controls arsenite oxidation in the chemolithoautotroph NT-26. *FEMS Microbiol Lett* **313:** 20–28.

Shen, S., Li, X.-F., Cullen, W.R., Weinfeld, M., and Le, *, X.C. (2013) Arsenic binding to proteins. *Chem Rev* **113:** 7769–7792.

Stock, J.B., Ninfa, A.J., and Stock, A.M. (1989) Protein phosphorylation and regulation of adaptive responses in bacteria. *Microbiol Rev* **53:** 450–490.

Somerville, J.E., and Kahn, M.L. (1983) Cloning of the glutamine synthetase I gene from *Rhizobium meliloti*. *J Bacteriol* **156:** 168–176.

Souza, V., Eguiarte, L.E., Siefert, J., and Elser, J.J. (2008) Microbial endemism: does phosphorus limitation enhance speciation? *Nat Rev Microbiol* **6:** 559–564.

Takeuchi, M., Kawahata, H., Gupta, L.P., Kita, N., Morishita, Y., Ono, Y., and Komai, T. (2007) Arsenic resistance and removal by marine and non-marine bacteria. *J Biotechnol* **127:** 434–442.

Van Bogelen, R.A., Olson, E.R., Wanner, B.L., and Neidhardt, F.C. (1996) Global analysis of proteins synthesized during phosphorus restriction in *Escherichia coli*. *J Bacteriol* **178:** 4344–4366.

Wanner, B.L. (1996) Phosphorous assimilation and control of the phosphate regulon. In: *Escherichia coli and Salmonella typhimurium Cellular and Molecular Biology*. Neidhardt, F.C., Curtiss, R.I., Ingraham, J.L., Lin, E.C., Low, K.B.J., Magasanik, B., *et al*. (eds). Washington, DC, USA: American Society for Microbiology, pp. 1357–1381.

Wang, Q., Qin, D., Zhang, S., Wang, L., Li, J., Rensing, C., McDermott, T.R., and Wang, G. (2015) Fate of arsenate following arsenite oxidation in *Agrobacterium tumefaciens* GW4. *Environ Microbiol* **17:** 1926–1940.

Wolfe-Simon, F., Blum, J.S., Kulp, T.R., Gordon, G.W., Hoeft, S.E., Pett-Ridge, J., *et al*. (2011) A bacterium that can grow by using arsenic instead of phosphorus. *Science* **332:** 1163–1166.

Yan, C., Wang, Z., and Luo, Z. (2014) Arsenic efflux from *Microcystis aeruginosa* under different phosphate regimes. *PLoS One* **9:** e116099.

Yang, H.C., and Rosen, B.P. (2016) New mechanisms of bacterial arsenic resistance. *Biomed J* **39:** 5–13.

Zavaleta-Pastor, M., Sohlenkamp, C., Gao, J.L., Guan, Z., Zaheer, R., Finan, T.M., *et al*. (2010) *Sinorhizobium meliloti* phospholipase C required for lipid remodeling during phosphorus limitation. *Proc Natl Acad Sci U S A* **107:** 302–307.

Supporting information

Additional Supporting Information may be found in the online version of this article at the publisher's web-site:

Table S1. Bacterial strains, plasmids and primers used in this study.

Fig. S1. Amino acid sequences of phylogenetically diverse PhoRs. Residues conserved across all sensor kinases are indicated by an asterisk. Phosphorylation sites H210 and the HATPase domain G359 and G361 are highlighted by the red boxes.

Fig. S2. SDS-PAGE illustration of His-tagged purified proteins over explained in *E. coli* and used in the phosphorylation assays. The sensor kinases PhoR and Aios are without the 5′ membrane spanning region, whereas the cognate response regulators PhoB1, PhoB2 and AioR are complete.

Fig. S3. Autophosphorylation of PhoR and AioS. Equal volume reaction aliquots taken at different time points (shown in minutes) were loaded into SDS-PAGE gels (shown at left) and Phos-tag SDS-PAGE gels (shown at right) and electrophoresed.